Breast imaging with ultrasound tomography: a comparative study with MRI

Bryan Ranger, Peter Littrup, Neb Duric, Cuiping Li, Steven Schmidt, Jessica Lupinacci, Lukasz Myc, Amy Szczepanski , Olsi Rama and Lisa Bey-Knight

Karmanos Cancer Institute, Wayne State University, 4100 John R. Street, Detroit, MI 48201

ABSTRACT

The purpose of this study was to investigate the performance of an ultrasound tomography (UST) prototype relative to magnetic resonance (MR) for imaging overall breast anatomy and accentuating tumors relative to background tissue. The study was HIPAA compliant, approved by the Institutional Review Board, and performed after obtaining the requisite informed consent. Twenty-three patients were imaged with MR and the UST prototype. T_1 weighted images with fat saturation, with and without gadolinium enhancement, were used to examine anatomical structures and tumors, while T_2 weighted images were used to identify cysts. The UST scans generated sound speed, attenuation, and reflection images. A qualitative visual comparison of the MRI and UST images was then used to identify anatomical similarities. A more focused approach that involved a comparison of reported masses, lesion volumes, and breast density was used to quantify the findings from the visual assessment. Our acoustic tomography prototype imaged distributions of fibrous stroma, parenchyma, fatty tissues, and lesions in patterns similar to those seen in the MR images. The range of thresholds required to establish tumor volume equivalency between MRI and UST suggested that a universal threshold for isolating masses relative to background tissue is feasible with UST. UST has demonstrated the ability to visualize and characterize breast tissues in a manner comparable to MRI. Thresholding techniques accentuate masses relative to background anatomy, which may prove clinically useful for early cancer detection.

Keywords: breast, lesion, cancer, ultrasound tomography, MRI

1. INTRODUCTION

Breast magnetic resonance imaging (MRI) is now recognized as an important adjunctive examination to mammography and ultrasound[1]. The utility of MR in investigating breast cancer is largely due to its capability to detect what other modalities miss[2]. By analyzing morphology and enhancement characteristics, it can successfully differentiate between benign and cancerous lesions[3]. However, MRI machines are extremely costly to house, require specialized staff for operation, and are known for their characteristically long scan times.

The above disadvantages have limited the use of MR in both screening and diagnosis[4]. Consequently, a modality that can rival MR's image quality while obviating these difficulties could potentially have a far greater societal impact. The experimental approach discussed in this paper made use of an Ultrasound Tomography (UST) device, which utilizes ultrasound transducer arrays to construct whole breast images from measurements of scattered acoustic pulses interacting with breast tissue[5]. Whole-breast analysis in a single scan allows for the extraction of diagnostic information from the entire volume of the breast. Such information is vital for tumor detection and characterization. Furthermore, the ability to accurately image and characterize breast anatomy with UST enables quantitative estimates of breast density, which has been linked to breast cancer risk, as initially described by Glide, Duric and Littrup[6],

Our primary objective was to determine whether UST can generate images comparable to MR. The ultimate goals of such a study are to provide both diagnostic accuracy aimed at reducing the biopsy rate of benign lesions and a means of characterizing masses within high-risk women that have denser breast tissue or fibrocystic changes. This pilot study compares MR imaging with UST for a cohort of 23 patients. The aims of the study are to establish quantitative UST thresholds for its new imaging parameters and to assess its clinical potential relative to MRI. To this end, we have

Medical Imaging 2010: Ultrasonic Imaging, Tomography, and Therapy, edited by Jan D'hooge, Stephen A. McAleavey,
Proc. of SPIE Vol. 7629, 762906 · © 2010 SPIE · CCC code: 1605-7422/10/$18 · doi: 10.1117/12.845650

examined similarities and differences between suspicious lesions and anatomical structures found in both imaging modalities through qualitative and quantitative comparisons. We also present a quantitative analysis comparing whole-breast dense tissue content from MRI and UST images.

2. METHODS

2.1 Patient Recruitment

All imaging procedures were performed under an Institutional Review Board-approved protocol, in compliance with the Health Insurance Portability and Accountability Act, with informed consent obtained from all patients. Twenty-three patients were imaged with both MR and the UST prototype. MR scans were received as axially oriented images which were then re-sliced using the public domain image analysis package, *ImageJ*[7], into coronal views to match the native format of the UST acquisitions. We used gadolinium-enhanced, fat-subtracted T_1-weighted images to define the volume and extent of cancers. T_2-weighted images were useful to define benign lesions such as cysts. Finally, our density study utilized T_1-weighted, pre-contrast images without fat saturation. The dataset represents a variety of breast shapes, patient ages, breast densities, and contains both benign and cancerous lesions.

2.2 UST Data Acquisition

The principles and techniques of the UST device are described in detail in previous publications[5]. The device is markedly different than that of other imaging modalities such as mammography and conventional ultrasound (Fig. 1). The patient lies in the prone position on the examination bed with the breast suspended through a hole in the thin, pliable sail cloth opening into a water tank. Water, due to its well-defined sound speed (~1.5 km/s) close to that of breast tissue, serves as the coupling medium between the breast and transducer. A ring transducer, operating at a central frequency of 2 MHz, encircles the breast and scans from the patient's chest wall to the nipple region by means of a motorized gantry. The transducer consists of 256 elements that both emit and receive the ultrasound signals. The acquisition time of a complete scan is approximately 1 minute and consists of 45-115 tomographic slices of the breast (depending on the breast size) at 1 mm intervals.

Three types of images are produced from the raw data using previously described tomographic reconstruction algorithms[8]: (i) sound speed, (ii) attenuation and (iii) reflection. *Sound speed* images are based on the arrival times of acoustic signals. Previous studies have shown that cancerous tumors have enhanced sound speed relative to normal breast tissue[9], a characteristic which can aid the differentiation of masses, normal tissue, and fat. *Attenuation* images are tomographic reconstructions based on acoustic wave amplitude changes. Higher attenuation in cancer causes greater scatter of the ultrasound (US) wave, so attenuation data in conjunction with sound speed provides a potentially effective means for determining malignancy. *Reflection* images, derived from changes of acoustic impedance, provide echo-texture data and anatomical detail for the entire breast. Reflection images are valuable for defining tumor margins which can be used to characterize lesions through the so called Stavros criteria[10]. These 3 types of images can be combined without geometric discrepancy by means of image fusion, allowing for multi-parameter visual and quantitative characterization of masses.

2.3 Image Analysis

A macro developed for *ImageJ* was used to fuse reflection (I_r), attenuation (I_a) and sound speed (I_s) UST images and to adjust image thresholds. Image fusion allows for improved visualization so that multiple characteristics can be viewed as one image, and breast tissue features can be evaluated more comprehensively. In addition to accentuating the lesion, the fused image depicts the local and distant tumor environment, including parenchyma and other components of breast

architecture. Parenchymal tissue was visualized by varying the rendered range of sound speeds in the UST images to match the appearance of parenchyma in the MRI images. Depiction of lesions was similarly optimized using a combination of sound speed and attenuation thresholds and comparing the results with DCE-MRI renderings of the same lesions at maximum enhancement. A final fused image was created by adding the reflection image, I_r, the thresholded sound speed image, I_s, and the combined sound speed and attenuation image, I_a, as indicated by the formula,

$$I_f = I_r + I_{s=a}^{s=b} + \left[I_{s>c} \bullet I_{a>d} \right],$$

where $\bullet$ denotes the logical .AND. operation, and *a,b,c,d* are variable threshold values.

The final image thereby displays breast architecture (via I_r), parenchyma (via I_s) and suspicious lesions (via $I_s \bullet I_a$), simultaneously. Gray-scale images, which are most comparable to MR, were used for direct visual comparison.

Similarities in the sensitivity and resolution of the two imaging modalities enables this fusion process. The spatial resolution of the MRI data is ~ 1 mm and the image slices are typically 1 mm thick. The UST images are characterized with an in-plane spatial of resolution of 1 to 2 mm with a slice thickness of ~ 4mm. All comparisons were made under the supervision of a radiologist with over 15 years of experience and a radiology resident. During the comparison process, the MR imaging parameters that were given particular consideration were (i) the estimated size of the primary tumor, (ii) the presence of additional suspicious lesions, (iii) the distribution of parenchymal and fibroglandular tissue. Furthermore, 3D projections of the lesions were created from the thresholded MRI and UST stacks for additional visual comparison. This function allowed us to rotate the masses so that the morphology and volume distribution of the lesions could be compared.

In order to compare masses rather than overall breast architecture we relied on the observation that masses tend to have higher sound speeds relative to background tissue. Starting with the threshold that emphasized anatomical equivalence between UST and MRI, we progressively increased the sound speed threshold until masses could be optimally isolated from background tissue. This procedure was repeated for the attenuation images. The thresholded images were then fused with the reflection image to show the isolated mass in relation to breast architecture. A "detected mass" by UST was defined as a distinct feature appearing in one or more UST modalities that coincided in location and size with masses identified in the corresponding MR images.

Once a preliminary relationship was suggested by visual assessment, a more quantitative technique was used to verify that UST was producing analogous images. A quantitative study also eliminated much of the subjectivity associated with visual analysis, and justified the reproducibility of our techniques. First, we obtained standard US and MRI reports to determine the number of reported masses. We then sought corresponding masses in the UST images. Ultrasound and pathology data were used to calibrate any systematic effects in tumor size caused by MR's tendency to overestimate tumor size relative to pathological measurements[11].

To estimate lesion volumes, we first obtained mass dimensions from the MRI reports. Employing the ellipsoid formula: $\pi/6$ x Length x Width x Height, we were able to approximate lesion volumes. To acquire lesion dimensions from MRI and UST, we used coronal views for the xy-plane, and an axial re-slice of the coronal image to acquire depth in the z-plane. All three images gathered from UST were used to gather dimensions. Following volume calculations and threshold determinations, we calculated the mean threshold in an attempt to determine whether a unique universally applicable threshold could be ascertained. Using the average thresholds for sound speed and attenuation, we recalculated the volumes of each mass using the mean thresholds to determine the variation of mean threshold acquired volumes from actual lesion volumes.

3. RESULTS

A final fused UST image was created by adding the reflection image, the thresholded sound speed image and the combined sound speed and attenuation image as discussed in the materials and methods section. The result of adjusting thresholds to match the MRI images yielded the following mean threshold values for delineating parenchyma and masses.

$$a = 1.43\,km/s, \quad b = 1.52\,km/s, \quad c = 1.52\,km/s, \quad d = 0.15\,dB/cm.$$

It was found that image pixels that simultaneously exceeded thresholds of 1.52 km/s for sound speed and 0.15 db/cm in attenuation, defined tumor extent, similarly to DCE-MRI.

A visual comparison of the fused UST images with the MRI sequences showed that the UST images were most comparable to the T_1 fat-subtracted gadolinium enhanced MRI sequences. A visual assessment of the images led to the identification of parenchyma, fibrous stroma, masses and fatty tissues in both UST and MR images. These components of breast anatomy were distributed in a similar manner in the two image sets (Fig. 2). The gray-scale in the fused image corresponded directly to the fat-subtracted MR image, where dark gray represented fat, light gray parenchyma, and the white bands fibrous stroma.

Benign masses tended to assume properties more similar to normal breast tissue. Consequently, their characterization relied heavily on the use of reflection images. Utilizing the reflection image as background in the fused image, cysts could be accentuated by clearly defined boundaries (Fig. 3). Parenchyma was also visible in the fused image and correlated closely to what was seen on MR. Other benign lesions, such as fibroadenomas, were visible in fused images when a low attenuation threshold was applied.

In the DCE-MRI images, suspicious masses were identified by their contrast enhancement. As described earlier, suspicious masses were visualized in the UST images as those regions that were above a certain threshold of attenuation (~0.15 dB/cm) and sound speed (~1.52 m/s), and displayed in color in the fused image. Such properties are consistent with dense, stiff masses, which often suggest malignancy[9]. Under such a methodology, a suspicious lesion can be isolated in UST images more consistently than the same lesion in non-contrast MR images. In Figure 4, both UST and DCE-MRI show masses of similar size and extent, located within identical quadrants of the breast. Furthermore, this figure emphasizes UST's ability to accurately image a carcinoma located within dense parenchymal tissue without the use of contrast enhancement. Other comparative examples of tumor detection are shown in figures 5 and 6. Comparison with contrast-enhanced fat-subtracted MR images shows that the UST-identified masses do indeed correspond to the masses identified in MR. In all cases when cancer was present within UST's scanning range, our fusion method was able to detect it.

Using the methodology described above for isolating a region of interest, we calculated lesion volumes from UST data by thresholding and dimensional analysis. The volumes obtained were compared to similarly determined volumes from MRI. The standard deviation of the volume differences for all masses, when comparing UST to MRI, was found to be 0.59 cm^3. The mean thresholds we obtained for sound speed and attenuation from calculations of tumor volume were 1.483 km/s and 0.176 dB/cm respectively. To determine if the mean thresholds could be applied as universal thresholds, we re-calculated all of the volumes using these 2 threshold values. The volumes deviated from the mean by 2.54 cm^3 and 6.43 cm^3 respectively. This result demonstrates that a universally applicable threshold may be able to determine tumor volume but with moderate variance. Further study with more patients is necessary to validate the universality of such threshold.

4. DISCUSSION

Fused UST images, rendered in grey-scale, show similar breast architecture as seen in T_1-weighted MR images. Any anatomical differences can be accounted for by (i) dissimilar breast deformation under MRI (air) and UST (water) examination conditions, (ii) lower spatial resolution of UST images and (iii) greater slice thickness associated with UST images. Color-coded thresholding of UST images enhanced the visibility of breast masses, particularly those deemed suspicious by DCE-MRI. The concordance of breast anatomy visualized by UST and MRI suggests that the effect of artifacts and errors associated with UST imaging are modest and do not limit the interpretation of the UST images. Furthermore, this concordance provides justification for pursuing the UST method with the goal of leveraging its lower intrinsic cost and short exam times.

It has been known for some time that mammographic breast density (determined form the distribution of radio-opaque regions on a mammogram) strongly correlates with breast cancer risk. However, mammography is not an ideal measurement tool because it provides only an areal measurement (not true density) and its ionizing radiation prevents its use in young patients. MRI is a better tool in that regard, but is very expensive, as noted above. Furthermore, in contrast to MR, UST provides an absolute quantitative scale which removes some of the subjectivity associated with reading MR

images and allows for further study in areas such as breast density. The concordance of UST and MRI images therefore suggests that UST may become a better tool for measuring breast density, the subject of a future paper.

We have had success in differentiating and depicting benign lesions (including complex cysts, simple cysts and fibroadenomas) and cancer from surrounding breast tissue. However, in order for fibroadenomas to be visible in our fused images, a lower attenuation threshold (~0.1 dB/cm) had to be applied as fibroadenomas normally exhibit high sound speed with little attenuation of the acoustic wave. If cancer was present and within scanning range, it was found using the described fusion methodology in all cases. Differentiation of malignant from parenchymal tissue was achieved in all patients without the use of contrast agents. This suggests that ultrasound tomography can successfully, even in women with dense breasts, detect and characterize various breast lesions in a completely non-invasive manner. Future studies utilizing microbubble-based contrast agent should further enhance the UST images and allow for added diagnostic accuracy.

In this study, the UST exams missed some of the unknown (secondary) masses if they fell outside of its scanning range. This occasionally occurred for women with large breasts for whom the scanning range had to be centered on the location of the known mass. This limitation is brought about by UST's initial storage memory of 11 Gb which limits the number of scans that can be acquired. This limitation has now been removed (memory is now 22 Gb) and should improve future studies. Future scans should have the capability to detect additional lesions beyond those found in this study. Although limited in scope, our study suggests that UST has the potential to find masses not detected by standard US and mammography exams.

5. CONCLUSIONS

Fused UST images, rendered in grey-scale, show similar breast architecture seen on T_1 weighted MRI images. Minor differences can be accounted for by the differing breast geometries and the lower spatial resolution of the UST images. Color-coded thresholding of UST images was shown to enhance the visibility of breast masses. The thresholded UST images are more effective in identifying masses than the T_1 weighted MRI images and are more similar to the contrast-enhanced, fat-subtracted MRI images. In conclusion, our pilot study has demonstrated a concordance between UST and MRI depictions of breast anatomy. Furthermore, there is a concordance between thresholded UST fused images and DCE-MRI for the detection of suspicious lesions. Thresholded UST images, therefore have the potential to provide an effective means for identifying breast masses. A strong correlation between UST and MRI rendered breast anatomy suggests that UST could provide a lower-cost alternative to MRI for volume based assessments of breast density. Future studies comprising a larger cohort of patients are planned to further characterize UST's sensitivity to breast masses and its role in measuring breast density.

6. ACKNOWLEDGMENTS

The authors acknowledge that this work was support by a grant from the Michigan Economic Development Corporation (Grant Number 06-1-P1-0653). For correspondence regarding this paper, contact Neb Duric at *duric@karmanos.org*.

7. REFERENCES

1. Schnall MD. Breast imaging technology: Application of magnetic resonance imaging to early detection of breast cancer. Breast Cancer Res 2001;3:17-21.
2. Lo G and Cheung PS. Use of magnetic resonance imaging for detecting clinically and mammographically occult ductal carcinoma in situ. Hong Kong Med J 2008;14(3):229-232.
3. MRI: Magnetic Resonance Imaging. Breastcancer.org Web site http://www.breastcancer.org/symptoms/testing/types/mri/. Accessed July 29, 2009.
4. Moore SG, Shenoy PJ, Fanucchi L, et al. Cost-effectiveness of MRI compared to mammography for breast cancer screening in a high risk population. BMC Health Serv Res. 2009;9:9.
5. Duric N, Littrup P, Poulo L, et al. "Detection of breast cancer with ultrasound tomography: First results with the computerized ultrasound risk evaluation (CURE) prototype," Med. Phys. 2007;34(2):773-85.
6. Glide-Hurst CK, Duric N, Littrup P., *Volumetric breast density evaluation from ultrasound tomography images.* Med Phys. 2008; **35**:pp. 3988-97.
7. ImageJ Web site. http://rsbweb.nih.gov/ij/. Accessed August 2, 2009.
8. Li C, **Duric N**, Littrup P, Huang L. In vivo breast sound-speed imaging with ultrasound tomography. *Ultrasound in Med. & Biol*., Vol. 35, 1615-1628, 2009.
9. Greenleaf JF, Johnson A, Bahn RC, and Rjagopalan B. "Quantitative Cross-sectional imaging of Ultrasound Parameters," 1977 Ultrasonics Symposium Proc., IEEE Cat. # 77CH1264-1SU, 989-995.
10. Stavros AT, Thickman D, Rapp CL, Dennis MA, Parker SH, Sisney GA. Solid breast nodules: use of sonography to distinguish between benign and malignant lesions. Radiology. 1995;196:123-34.
11. Onesti JK, Mangus BE, Helmer SD, et al. Breast caner tumor size: correlation between magnetic resonzne imaging and pathology measurements. Am J Surg 2008;196:844-850.

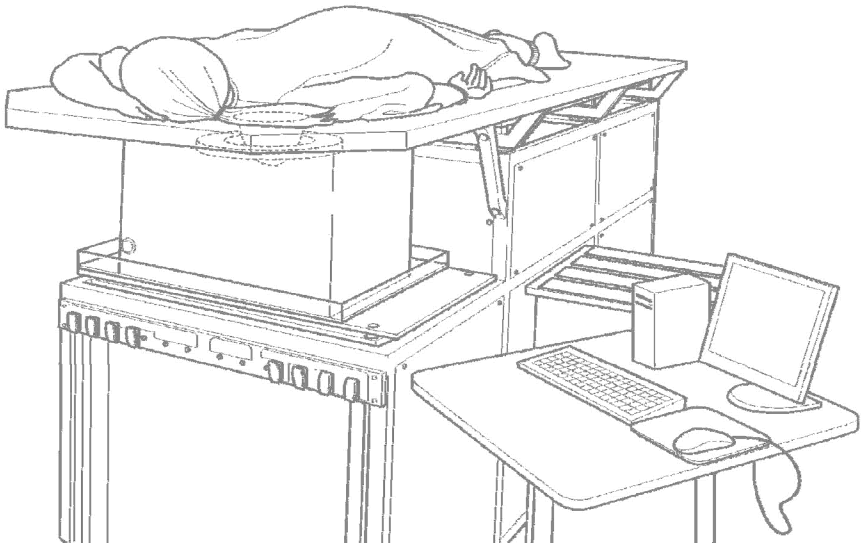

Figure 1: *Left*: UST clinical prototype with patient bed and system workstation. The patient lies face-down on the bed, with the breast suspended through the hole in the sail cloth. *Right*: The imaging tank which contains the ring transducer and mechanical gantry for scanning. The tank is filled with degassed water, set to body temperature.

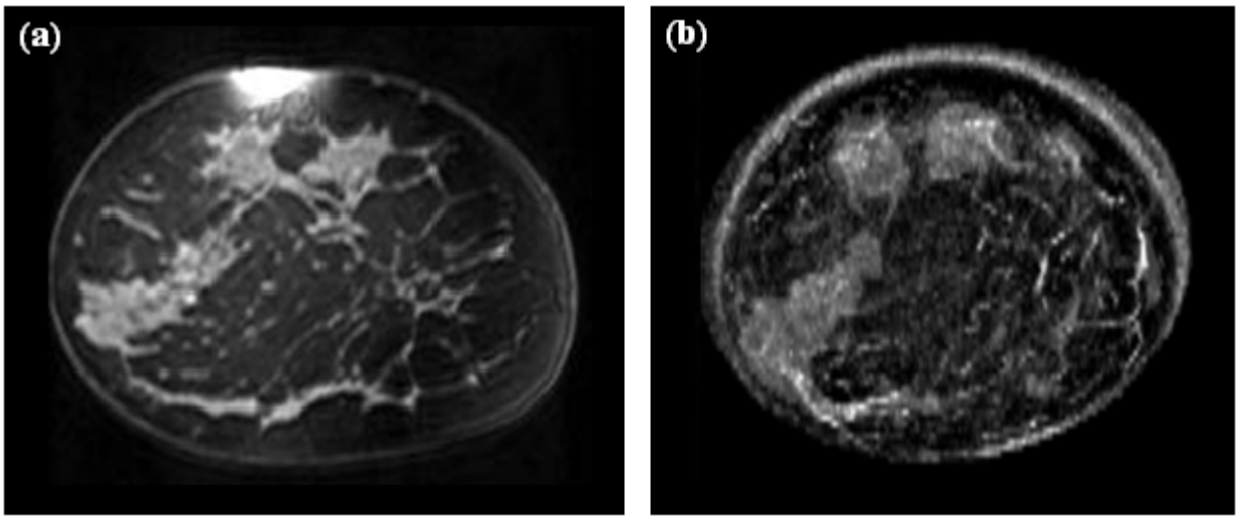

Figure 2: (a) Coronal fat-subtracted MRI image of breast. (b) Fused image, created using *ImageJ*, of the same patient. The anatomical features of the breast, especially the shape of the parenchyma, in the UST image and in the MRI image is almost identical. The dark gray corresponds to fat, the lighter gray represents the parenchyma, and the thin white bands are fibrous stroma.

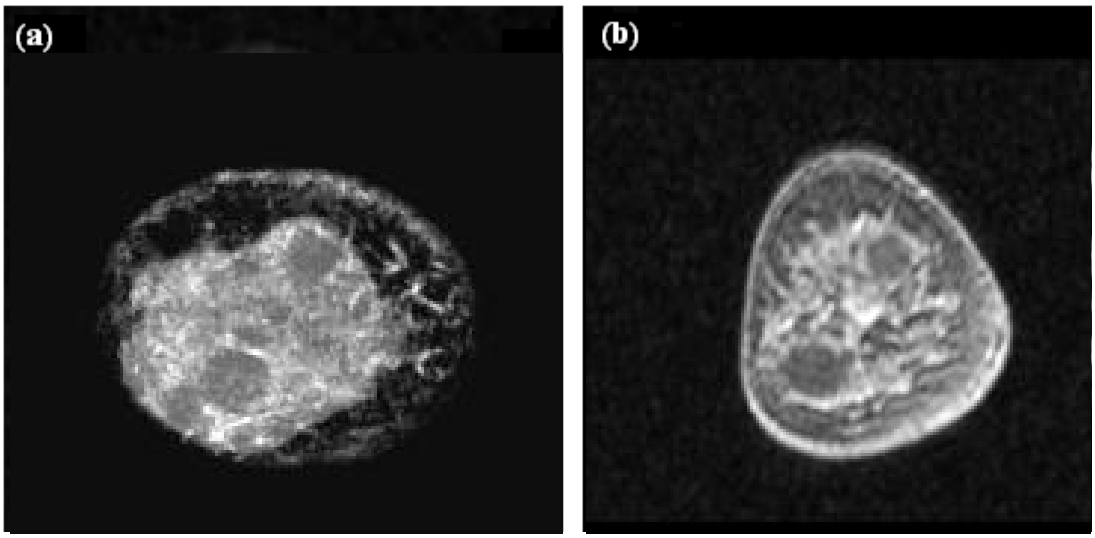

Figure 3: (a) Fused UST image, created using *ImageJ* . The UST shows the boundaries of all three benign lesions along with the parenchyma. Two simple cysts and one complex cyst are present. (b) Coronal fat-subtracted MRI image of breast for comparison.

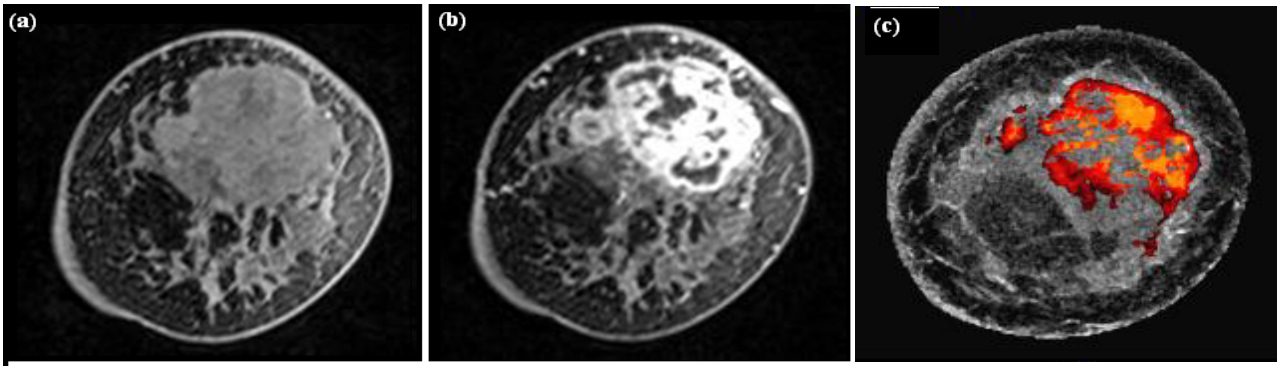

Figure 4: (a) Coronal T1 fat-subtracted MRI sequence prior to enhancement. (b) Contrast enhanced, fat-subtracted MRI image highlighting a large malignant mass. (c) Fused image. The colored area on the UST image shows that the mass has high sound speed and attenuation and closely correlates to the contrast enhanced image shown in (b).

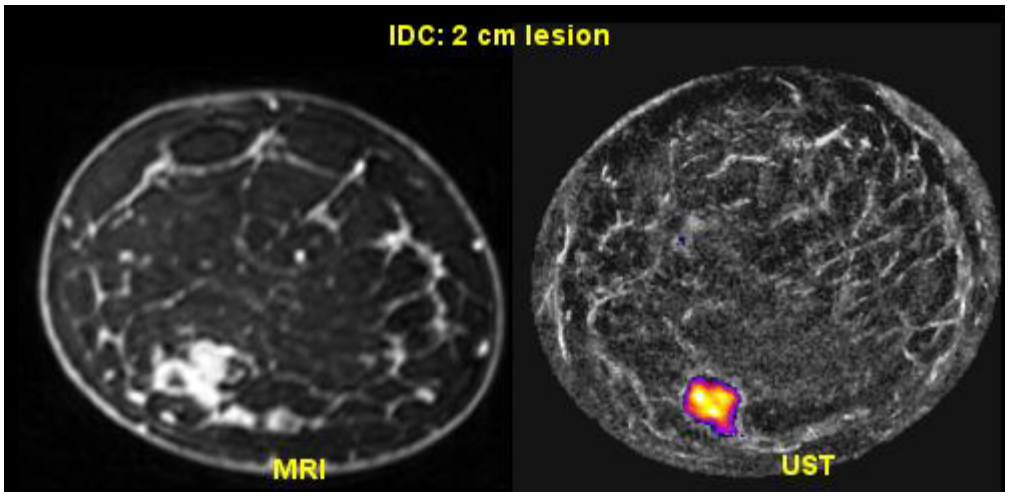

Figure 5: (a) Contrast enhanced, fat-subtracted MRI image highlighting a 2 cm malignant mass. (b) Fused UST image. The colored area on the UST image shows that the mass has high sound speed and attenuation and closely correlates to the contrast enhanced image shown in (a).

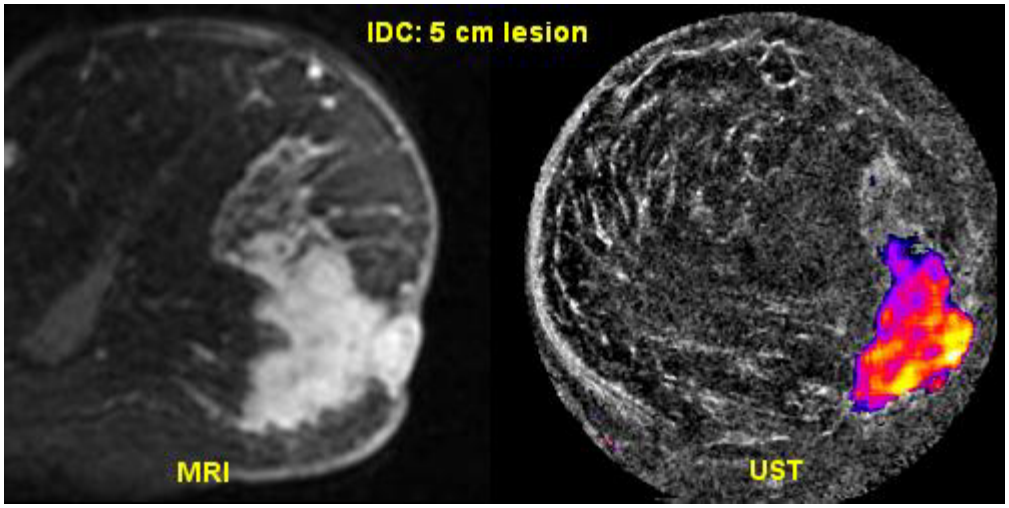

Figure 6: (a) Contrast enhanced, fat-subtracted MRI image highlighting a large malignant mass. (b) Fused UST image. The colored area on the UST image shows that the mass has high sound speed and attenuation and closely correlates to the contrast enhanced image shown in (a).